Suspended sediment properties and suspended sediment flux estimates in an inundated urban environment during a major flood event

Richard Brown[1] and Hubert Chanson[2]

Received 10 May 2012; revised 14 October 2012; accepted 15 October 2012; published 20 November 2012.

[1] During a major flood event, the inundation of urban environments leads to some complicated flow motion most often associated with significant sediment fluxes. In the present study, a series of field measurements were conducted in an inundated section of the City of Brisbane (Australia) about the peak of a major flood in January 2011. Some experiments were performed to use ADV backscatter amplitude as a surrogate estimate of the suspended sediment concentration (SSC) during the flood event. The flood water deposit samples were predominantly silty material with a median particle size about 25 μm and they exhibited a non-Newtonian behavior under rheological testing. In the inundated urban environment during the flood, estimates of suspended sediment concentration presented a general trend with increasing SSC for decreasing water depth. The suspended sediment flux data showed some substantial sediment flux amplitudes consistent with the murky appearance of floodwaters. Altogether the results highlighted the large suspended sediment loads and fluctuations in the inundated urban setting associated possibly with a non-Newtonian behavior. During the receding flood, some unusual long-period oscillations were observed (periods about 18 min), although the cause of these oscillations remains unknown. The field deployment was conducted in challenging conditions highlighting a number of practical issues during a natural disaster.

Citation: Brown, R., and H. Chanson (2012), Suspended sediment properties and suspended sediment flux estimates in an inundated urban environment during a major flood event, *Water Resour. Res.*, *48*, W11523, doi:10.1029/2012WR012381.

1. Introduction

[2] The vulnerability of urban environments with respect to flooding has been a long-standing concern of society [*Yevjevich*, 1992; *Ntelekos et al.*, 2008]. The inundation of urban environments leads to some complicated flow motion associated with significant sediment fluxes evidenced by the brownish color of the waters. Some key parameters are the suspended sediment concentration (SSC) and suspended sediment flux. The development of acoustic Doppler velocimetry (ADV) allowed the simultaneous measurements of instantaneous velocities and acoustic backscatter amplitude with relatively high temporal and spatial resolution, the latter being linked with the small control volume size. The backscatter amplitude may be related to the instantaneous suspended sediment concentration, although with proper calibration [*Fugate and Friedrichs*, 2002; *Nikora and Goring*, 2002; *Voulgaris and Meyers*, 2004].

[3] In the present study, the authors deployed an ADV unit in an inundated urban environment during a major flood of the Brisbane River in January 2011, and they investigated the relationship between ADV backscatter amplitude and suspended sediment concentration. Flood deposit materials were collected in an inundated urban environment during the flood event to characterize the sediment properties. The aim of the study was to collect field measurements in a flooded urban setting and to characterize the suspended sediment flux. The results included the simultaneous measurements of turbulent velocities, SSC, and suspended sediment flux at high frequency for several hours about the peak of the flood.

2. Methods, Physical Environment, and Instrumentation

[4] The Central Business District (CBD) of the City of Brisbane is located on the left bank of the Brisbane River (Figures 1 and 2). Figure 1a is a map of the Brisbane River catchment, Figure 1b shows a map of the Brisbane River course through the City of Brisbane and Figure 2 presents an aerial view of the city center highlighting the 2011 field site location (red arrow). The city center is located 22 to 24 km upstream of the river mouth within the estuarine zone and the catchment area is 13,500 km^2. Between November 2010 and January 2011, some intense

[1]Faculty of Built Environment and Engineering, Queensland University of Technology, Brisbane, Queensland, Australia.
[2]School of Civil Engineering, University of Queensland, Brisbane, Queensland, Australia.

Corresponding author: H. Chanson, School of Civil Engineering, University of Queensland, Brisbane, Qld 4072, Australia. (h.chanson@uq.edu.au)

0043-1397/12/2012WR012381

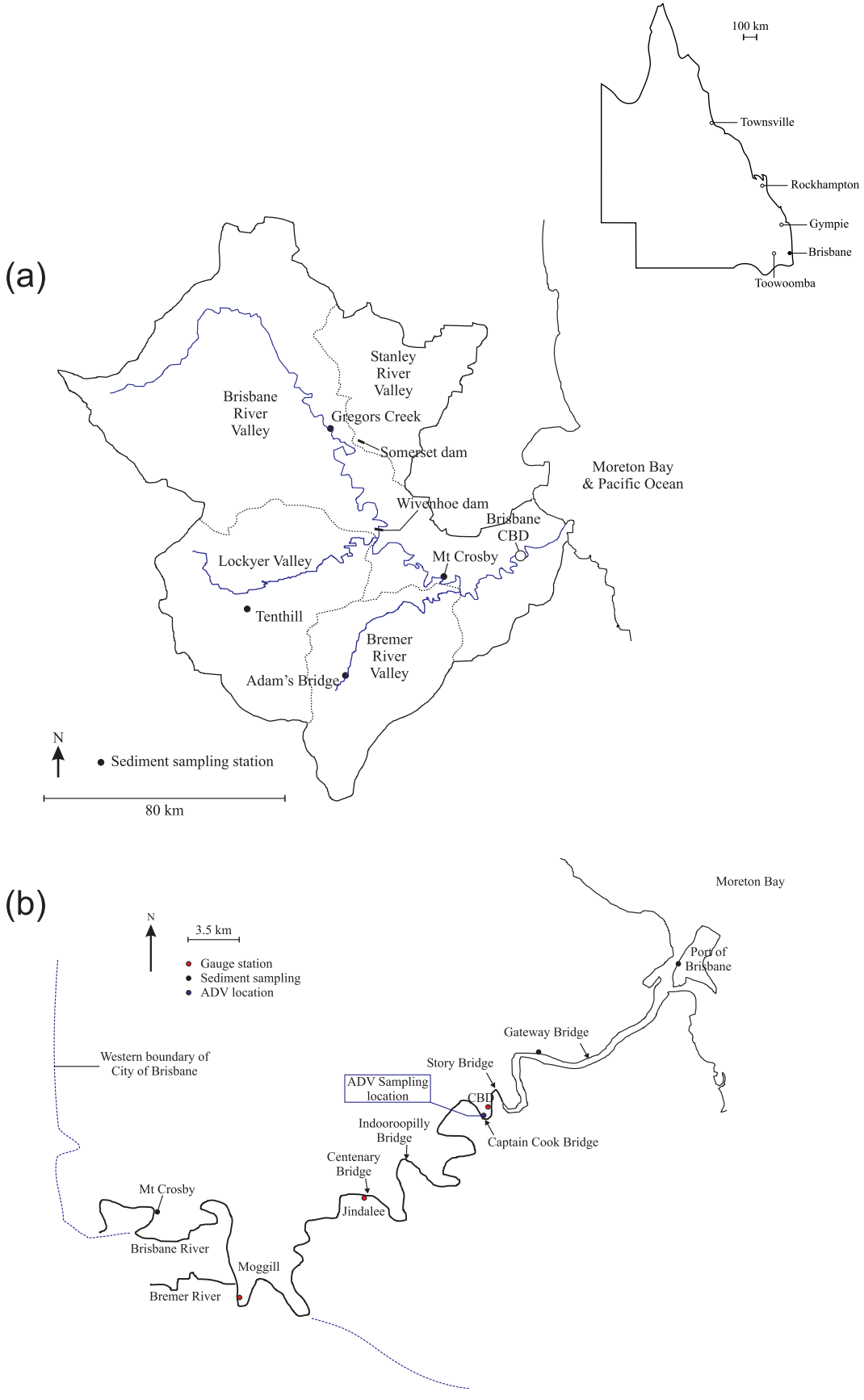

Figure 1. Map of the Brisbane River (Australia). (a) Map of the Brisbane River catchment (inset: map of Queensland). The Brisbane CBD is shown with a white dot and some upstream sediment sampling sites are shown with a black dot. (b) Map of the lower Brisbane River through the City of Brisbane (Australia). The sampling site is shown with a blue dot and the river gauge locations are shown in red.

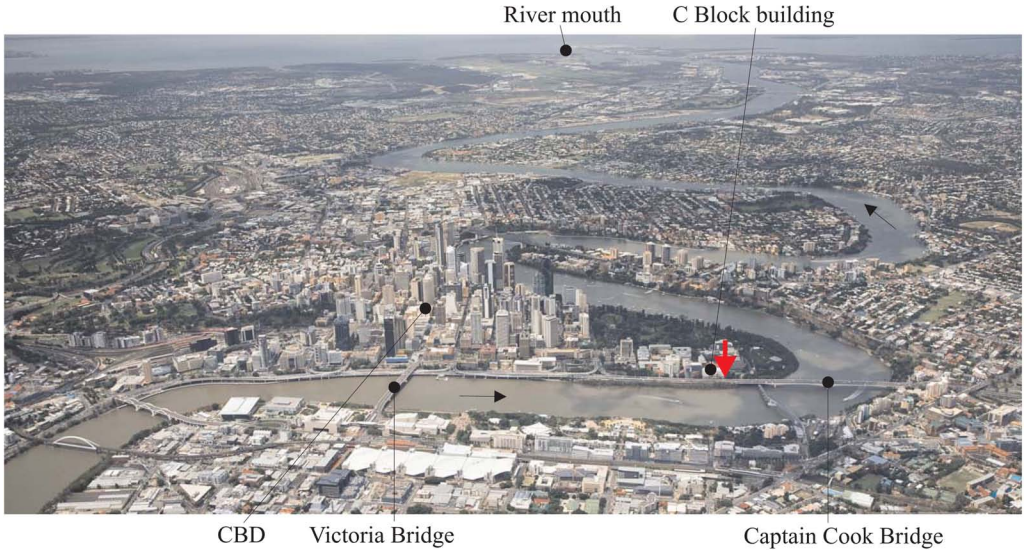

Figure 2. Brisbane River meanders between the city (foreground) and river mouth (background) in 2007 looking northeast. Black arrows show the main river direction. The red arrow points to the sampling site.

rainfalls were recorded across eastern Australia [*BOM*, 2011a,; *Chanson*, 2011]. In January 2011, the City of Brisbane experienced a major flood as the result of a combination of a heavily soaked catchment after a couple of months of rain, some heavy continuous rainfalls during the first two weeks of January 2011 in the whole Brisbane River catchment, and some intense rainstorm events over the upper and middle catchments on 10 and 11 January 2011 [*BOM*, 2011a]. All these induced some major flooding in Brisbane with the flood waters peaking on 12 January afternoon and 13 January early morning (Figure 3). The January 2011 flood caused the first major inundation of the City of Brisbane in 38 years, and the second major inundation in over 100 years. Figure 3 presents the flood hydrograph at three gauging stations located at 23, 49, and 71 km upstream of the river mouth; all elevations were measured above the Australian height datum (AHD). The gauge stations are shown in Figure 1b.

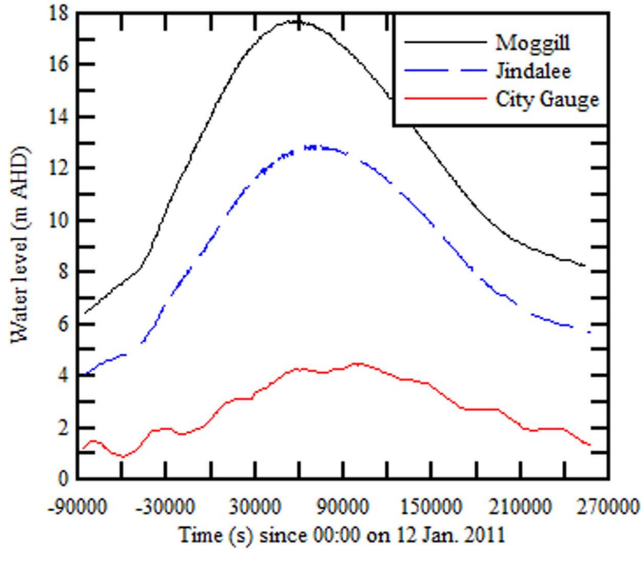

Figure 3. Flood hydrograph of the Brisbane River in 2011 at the Brisbane City Gauge, Jindalee, and Moggill located, respectively, about 23, 49, and 71 km upstream of river mouth.

[5] On 12 to 14 January 2011, an acoustic Doppler velocimeter SonTek^{TM} microADV (16 MHz, Serial No. A843F) was deployed in the inundated Gardens Point Road (Table 1 and Figure 4). The ADV unit was equipped with a three-dimensional-side-looking head. The ADV system was sampled at 50 Hz. Figure 4 presents the field site showing Gardens Point Road during and after the flood (Figures 4a and 4b), and a three-dimensional sketch of the ADV location relative to the adjacent car park (Figure 4c). Gardens Point Road was flooded from the morning of Wednesday 12 January 2011 till the early hours of Friday 14 January 2011. During the study period, the air temperature ranged between 18 and 27°C [*BOM*, 2011b]. At the sampling site during the study period, the water depth ranged between about 1 m and zero when the flood receded. This site was located between a busy access road and a car park during normal weather conditions; it was not a permanent monitoring site. All the ADV data underwent a thorough post-processing procedure to eliminate any erroneous or corrupted data from the data sets to be analyzed. The post processing included the removal of communication errors, the removal of average correlation values less than 60% [*McLelland and Nicholas*, 2000] and the removal of average signal-to-noise ratio (SNR) data less than 5 dB. Herein a 5 dB SNR threshold was selected because the SNR was observed to decrease sharply for suspended sediment concentrations (SSCs) greater than 40 kg m^{-3}. The accuracy on the ADV velocity measurements was 1% of the velocity range (2.5 and 1 m s^{-1}) [*Sontek*, 2008]. Further details were reported by *Brown et al.* [2011].

[6] Some sediment material was collected next to the sampling site about the high water line on 13 January 2011 midmorning and on 14 January 2011 early morning. The flood water deposit samples consisted of silty materials. A

Table 1. Turbulent Velocity Measurements in an Urban Environment of the Brisbane River Flood Plain on 12–13 Jan 2011[a]

Data File	ADV Location	Sampling Rate (Hz)	Velocity Range (m s^{-1})	Start Time (LT)	Duration	z (m)	V_x Direction	Comments
T1	A	50	2.5	12/01/2011 at 20:10:31	23 min 24 s	0.350	160.8°	Short ADV test.
T2	A	50	2.5	12/01/2011 at 20:40:08	4 h 26 min 40 s	0.350	160.8°	Test stopped when ADV dislodged by timber log and cable became entangled in rubbish bin wheel.
T3	B	50	2.5	13/01/2011 at 11:34:28	10 min 23 s	0.083	172.2°	Short ADV test.
T4	B	50	1.0	13/01/2011 at 12:08:55	3 h 48 min 38 s	0.083	172.2°	Test stopped to swap generator.
T5	B	50	1.0	13/01/2011 at 17:34:40	1 h 5 min 35 s	0.083	172.2°	Test stopped when water level dropped below the upper ADV receiver.

[a]Location A: ADV unit mounted horizontally on boom gate support (Figure 4). Location B: ADV unit mounted vertically on a hand rail (Figure 4). V_x direction: Mean longitudinal flow direction at the sampling location relative to the geographic north. z: Vertical elevation above the invert.

series of laboratory tests were conducted to characterize the bed material, i.e., the particle size distribution, organic content, rheometry, and acoustic backscatter properties. The soil sample granulometry was measured with a Malvern^{TM} laser sizer with duplicate measurements [*Shi*, 2011]. Note that no specific procedure was introduced to break the flocs. The fraction of organic content was determined by loss on ignition tests. The samples were oven dried at 105°C for 48 h before being allowed to cool down to room temperature; the subsamples were heated to 300°C for 2 h and then to 780°C for 1 h [*Schumacher*, 2002]. The rheological properties of flood water deposits were tested with a Mettler^{TM} 180 viscometer with a clearance of 0.59 mm between the two cylinders. The tests were repeated for a range of sample dilutions and analyzed following *Shi and Napier-Munn* [1996].

[7] The calibration of the ADV in terms of SSC was accomplished by measuring the signal amplitude of known, artificially produced concentrations of material obtained from the flood water deposit, diluted in tap water, and thoroughly mixed. All the experiments were performed on 18 January 2011. The laboratory experiments were conducted with the same SonTek^{TM} microADV system using two settings, identical to those used during the field observations on 12 to 14 January 2011. For each test, a known mass of sediment was introduced in a water tank which was continuously stirred with a paint mixer. The mixer speed was adjusted during the most turbid water tests to prevent any obvious sediment deposition on the tank bottom. The mass of wet sediment was measured with a Kern^{TM} PCB2000–1 (Serial No. WD080016381) balance, and the error was less than 0.1 g. The mass concentration was deduced from the measured mass of wet sediment and the measured water tank volume. During the tests, the suspended sediment concentrations ranged from less than 0.03 to 98 kg m^{-3}.

3. Results

3.1. Sediment Properties

[8] The sampled flood deposits were basically classified as cohesive mud. The relative density of wet sediment samples was about $\mathbf{s} = 1.461$, corresponding to a sample porosity of 0.72 assuming a relative sediment density of 2.64 [*Morris and Lockington*, 2002; *Shi*, 2011]. The particle size distribution data are presented in Figure 5 and the grain size statistics are summarized in Table 2 (columns 7 to 10). Figure 5 includes both the probability distribution and cumulative probability distribution functions (PDF) of four flood water deposits. The results were close considering that they were collected over two different days at four different locations (Table 2). The median particle size was in the silt size range with an approximate diameter of 25 μm [*Graf*, 1971; *Julien*, 1995; *Chanson*, 2004] and the sorting coefficient $\sqrt{d_{90}/d_{10}}$ ranged from 4.6 to 6.6 (Table 2). For comparison, some sediment samples collected in the Brisbane River are included in Table 2: The data indicated a median particle size ranging from about 5 μm to more than 1 mm (Table 2). Suspended sediment sampling in a number of Queensland rivers yielded a median particle size between 4 and 16 μm during small to moderate floods [*Horn et al.*, 1998]. The present particle size data were comparable to suspended sediment sample data collected during the flood events despite the different systems.

[9] The fraction of organic carbon in the flood water deposits was about 8%–9% on average (Table 2, column 9). For comparison, *Morris and Lockington* [2002] sampled the Brisbane River bed materials during a dry period and measured an organic carbon fraction ranging from 0.63% to 1.8%. The 2011 flood sediment data showed comparatively larger organic contents.

[10] The rheometry tests provided some information on the apparent yield stress τ_c and effective viscosity μ of the mud sludge as functions of the sample density. Herein only a rapid but also approximate characterization of the sediment material was performed (Figure 6a). The yield stress and apparent viscosity were estimated during the unloading phase by fitting the rheometer data with a Herschel-Buckley model, to be consistent with earlier studies [*Roussel et al.*, 2004; *Chanson et al.*, 2006a, 2011]. In a Herschel-Bulkley fluid, the relationship between shear stress τ and shear rate $\partial V/\partial z$ is assumed to be

$$\tau = \tau_c + \mu\left(\frac{\partial V}{\partial z}\right)^m, \quad (1)$$

where $0 < m < 1$ [*Huang and Garcia*, 1998; *Wilson and Burgess*, 1998]. For $m = 1$, equation (1) yields the Bingham fluid behavior, and a Newtonian behavior for $m = 1$ and $\tau_c = 0$. The experimental results are presented in Figure 6 and Table 3. The behavior of mud material highlighted some differences between the loading and unloading sequences (Figure 6a). For shear rates $\partial V/\partial z$ larger than 300 s^{-1}, the loading and unloading tests gave close results, suggesting a conservation of the macroscopic structure

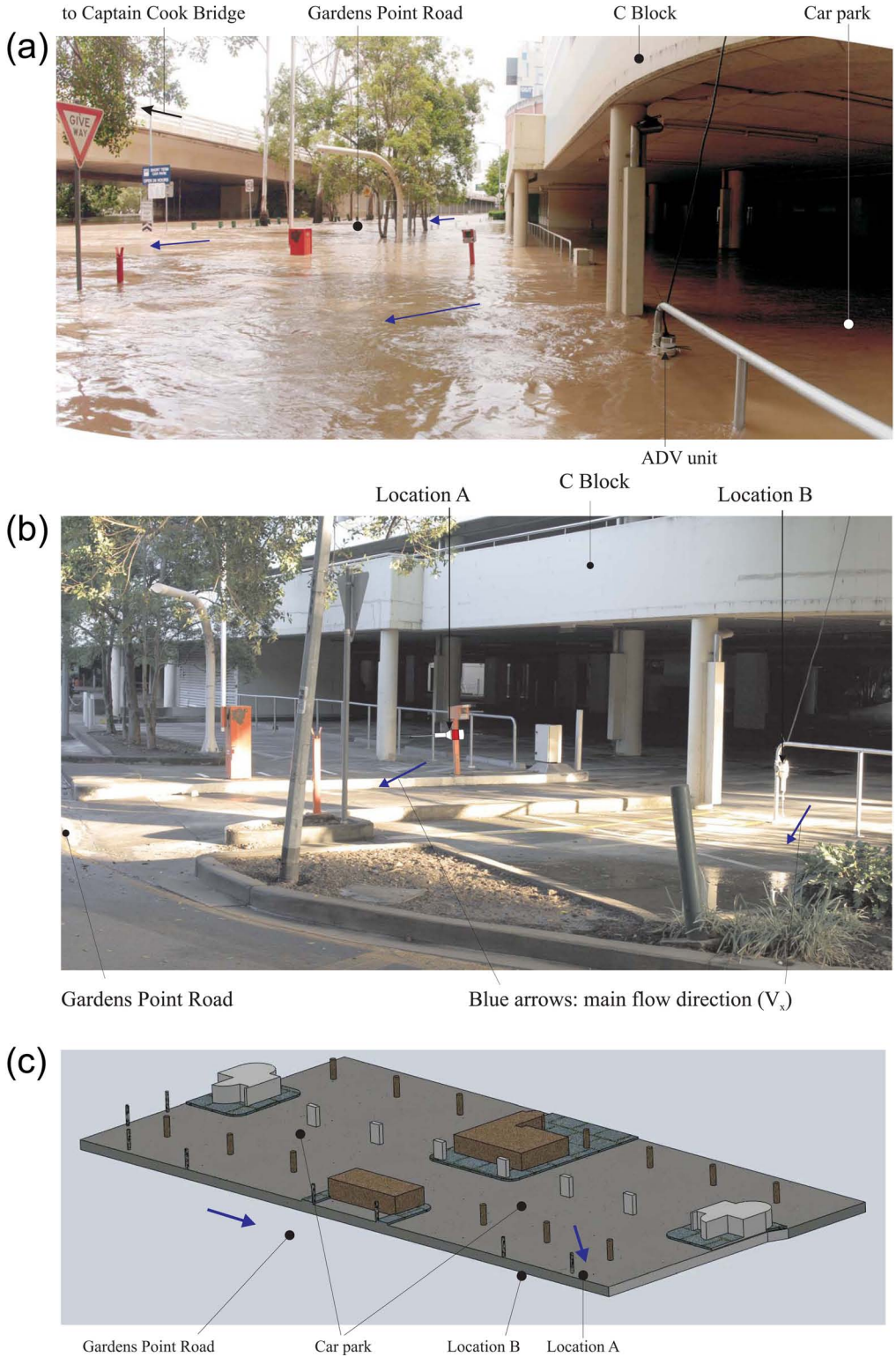

Figure 4. Field study in Gardens Point Road on 12–13 January 2011. The blue arrows show the main flow direction. (a) Inundated Gardens Point Road and C block building car park on 13 January 2011 at 11:40 (LT). Looking upstream at the flood flow. (b) Gardens Point Road and C block building car park on 14 January 2011 at 06:00. Note that both Gardens Point Road and C block building car park were cleaned up from any mud deposit during the night before. The ADV locations are highlighted. (c) Three-dimensional sketch of the C block building car park looking north.

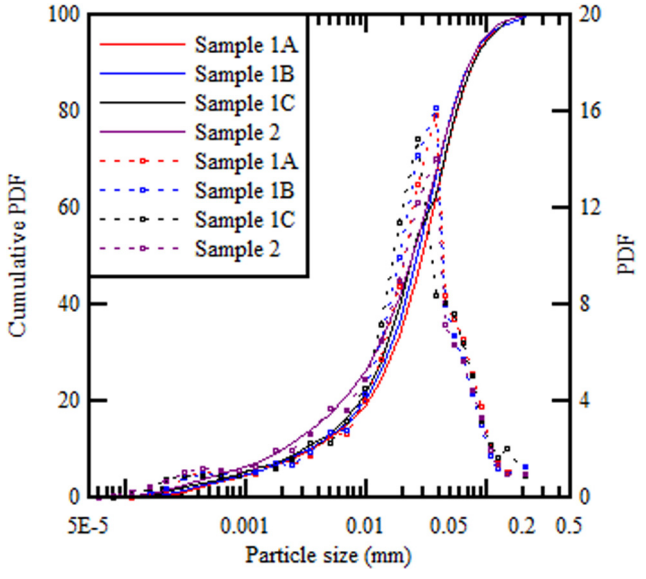

Figure 5. Particle size distributions of Brisbane River flood water deposit samples collected along Gardens Point Road on 13 and 14 January 2011: Probability distribution function (PDF) and cumulative probability distribution function.

possibly in the form of particle arrangement into thin layers. For the tests with the undiluted sediment sample (V2A), the apparent viscosity was $\mu = 8.1$ Pa s, the yield stress was about $\tau_c = 35.3$ Pa, and the exponent was $m = 0.34$. The results are compared with sediment mud samples collected in the Garonne River estuarine zone in Table 3 (columns 7 to 9). Figure 6b shows further the effects of dilution rate (or sample solid fraction) on the apparent yield stress τ_c and effective viscosity μ of the mud sludge.

[11] The rheometry results provided a characterization of the material yield stress, which is related to the minimum boundary shear stress required to erode and resuspend the sediments [*Otsubo and Muraoko*, 1988]. Furthermore, at high suspended sediment concentrations, the present results implied that the flood waters might exhibit some non-Newtonian characteristics, and their behavior cannot be predicted accurately without a rheological characterization of the sediment materials [*Wang et al.*, 1994; *Antoine et al.*, 1995; *Coussot*, 1997].

3.2. Acoustic Backscatter Amplitude and Suspended Sediment Concentration Calibration

[12] The relationship between acoustic backscatter amplitude (Ampl) and suspended sediment concentrations (SSC) was tested in laboratory for SSCs between 0 and 98 kg m^{-3}. The experimental results are summarized in Figure 7a. First the overall trend was independent of the ADV settings. No qualitative difference was observed between the two ADV settings. Second there was a good agreement between all data showing two characteristic trends. For SSC $\leq$ 3.2 kg m^{-3}, the data yielded a monotonic increase in suspended sediment concentration with increasing backscatter signal amplitude. A similar finding was discussed by *Fugate and Friedrichs* [2002] and *Chanson et al.* [2008] at low SSCs. For small

Table 2. Characteristics of Flood Water Deposits Collected in the Brisbane River: Flood Sediment Deposit Samples Collected in Gardens Point Road Next to C Block on 13 and 14 Jan 2011 (Present Study), and Comparison With Other Data Sets[a]

Reference	River	Sediment Sample	Location	Collection Date	Type	d_{50} (μm)	d_{10} (μm)	d_{90} (μm)	d_{90}/d_{10}	Percent Organic Carbon (%)	Remarks
Present Study	Brisbane River	Sample 1A	High waterline at roundabout, end of Gardens Point Rd	13 Jan 2011	Silt	29.4	3.54	75.9	21.4	8.2	Flood Deposits[b]
		Sample 1B	Concrete footpath beside ADV location B	13 Jan 2011	Silt	26.7	3.36	88.0	26.2	13.8	
		Sample 1C	Garden bed beside ADV location B	13 Jan 2011	Silt	24.6	2.93	91.5	31.2	6.4	
		Sample 2	B block parking ramp, Gardens Point Rd	14 Jan 2011	Silt	24.6	2.02	88.4	43.8	8.6	
Morris and Lockington [2002]	Brisbane River	Sample 1	BP Wharf (AMTD 2 km)	2001	Clayey sand	108.6	–	277.1	–	0.63	Dredged Materials
		Sample 2	Cairncross Dock (AMTD 12.9 km)	2001	Organic silt	<1.2	–	23.2	–	1.80	
Grinham (pers. commun.)	Brisbane River		Port of Brisbane (AMTD 1.1 km)	Sept 2007	–	12.3	3.36	64.29	19.2	–	Sediment Interface
			Hamilton Wharf (AMTD 12 km)	Sept 2007	–	17.6	3.66	136.9	37.4	–	
Grinham (pers. commun.)	Brisbane River		Mt Crosby weir (AMTD 90.8 km)	11 Feb 2011	–	4.8	0.6	21.9	36.5	–	Suspended Sediments[b]

[a]AMTD: adopted middle thread distance, measured upstream from the river mouth.
[b]No specific procedure was introduced to break the flocs. –: Data not available.

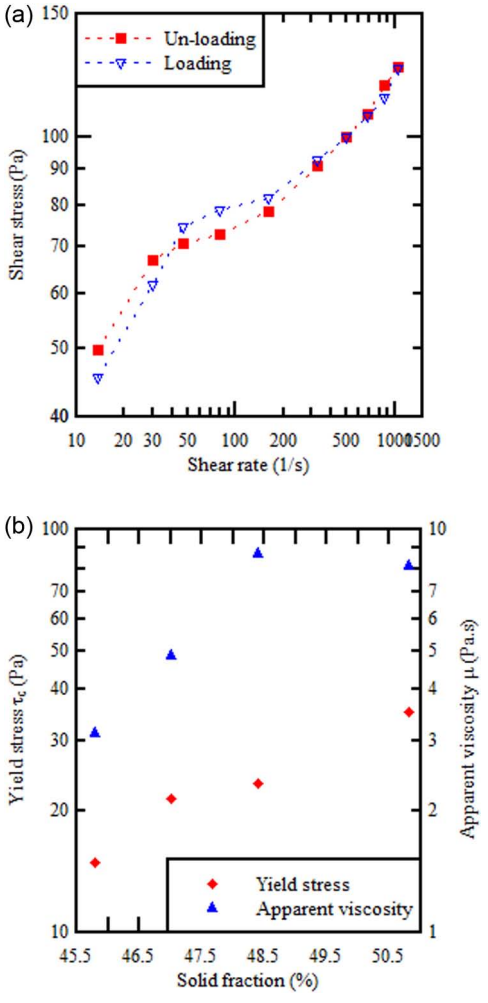

Figure 6. Results of mud/silt sample rheometry tests. (a) Loading and unloading cycle for sample V2A (original sample). (b) Effect of the solid fraction on the yield stress τ_c and apparent viscosity μ.

SSCs (SSC $<$ 3.2 kg m^{-3}), the data were independent of the ADV settings, and the best fit relationship was

$$\text{SSC} = 9.354 \times 10^{-3} \times e^{0.3009 \times (\text{Ampl} - 100.56)}, \quad \text{SSC} \leq 3.2 \text{ kg m}^{-3}, \tag{2a}$$

where the suspended sediment concentration SSC is in kg m^{-3} and the amplitude Ampl is in counts, and with a normalized correlation coefficient of 0.994. For larger SSCs (i.e., SSC $>$ 3.2 kg m^{-3}), the experimental results demonstrated a decreasing signal amplitude with increasing SSC. The results showed a good correlation between acoustic backscatter strength and SSC, although the ADV signal was saturated as previously observed by *Ha et al.* [2009] and *Chanson et al.* [2011]:

$$\text{SSC} = 54.23 - 0.4113 \times \text{Ampl} + \frac{25518}{\text{Ampl}^2}, \quad \text{SSC} > 3.2 \text{ kg m}^{-3} - \text{Velocity Range}: 1.0 \text{ m s}^{-1}, \tag{2b}$$

$$\text{SSC} = 72.61 - 0.6174 \times \text{Ampl} + \frac{81229}{\text{Ampl}^2}, \quad \text{SSC} > 3.2 \text{ kg m}^{-3} - \text{Velocity Range}: 2.5 \text{ m s}^{-1}, \tag{2c}$$

with a normalized correlation coefficient of 0.980 and 0.999, respectively. Equations (2) are compared with the data in Figure 7a.

[13] It is shown in section 3.3 that the SSCs were greater than 3 kg m^{-3} during the field study, and equations (2b) and (2c) were used to estimate the suspended sediment concentration from the signal amplitude.

3.3. Field Measurements of Instantaneous Velocity, SSC, and Suspended Sediment Flux

[14] On 12–14 January 2011, the field measurements were conducted in an inundated section of the city center. The present study did not yield a continuous data set because of a number of practical issues experienced during the investigation. At the end of the second deployment (data file T2; Table 1), the ADV unit was found held solely by its cable. It is believed that the ADV was first dislodged by the impact of a timber log and, later, a rubbish bin wheel became entangled in the ADV cable. On the morning of 13 January 2011, the ADV unit was repositioned to a nearby handrail and mounted vertically (location B). During the fourth deployment (data file T4; Table 1), the ADV unit had to be stopped because the generator was required to assist flood victims. The fifth and final deployment (data file T5; Table 1) ended when the flood waters receded and the upper ADV receiver came to be out of the water. After the ADV was dislodged by impact (data file T2), the ADV unit was inspected, checked, and tested (test T3). While the test results were successful, an inspection of the ADV system revealed that the stem was very slightly bent. The authors acknowledge that this physical damage might have some effect on the ADV data, although a careful data analysis of tests T3, T4, and T5 shows no obvious problem.

Table 3. Measured Properties of Mud Samples: Brisbane River Flood Water Deposits Collected Along Gardens Point Road Next to C Block on 14 Jan 2011 (Present Study) and Mud Samples Collected in the Garonne River Estuarine Zone [*Chanson et al.*, 2011][a]

Study	Sample Number	Sample Ref.	Description	s	Solid Fraction	τ_c (Pa)	μ (Pa)	m
Brisbane River	Sample 2	V2A	Brisbane River Sediment	1.461	0.508	35.32	8.10	0.342
		V2B	Diluted (+15 g water)	1.439	0.484	23.36	8.68	0.308
		V2C	Diluted (+30 g water)	1.418	0.470	21.41	4.84	0.347
		V2D	Diluted (+45 g water)	1.400	0.458	14.89	3.13	0.360
Garonne River	Sample 1	Test2	Arcins Channel Sediment	1.41	–	49.7	44.7	0.277
	Sample 2	Test3	Arcins Channel Sediment	1.41	–	61.4	55.9	0.273

[a]**s** is wet sediment sample relative density. –: Data not available.

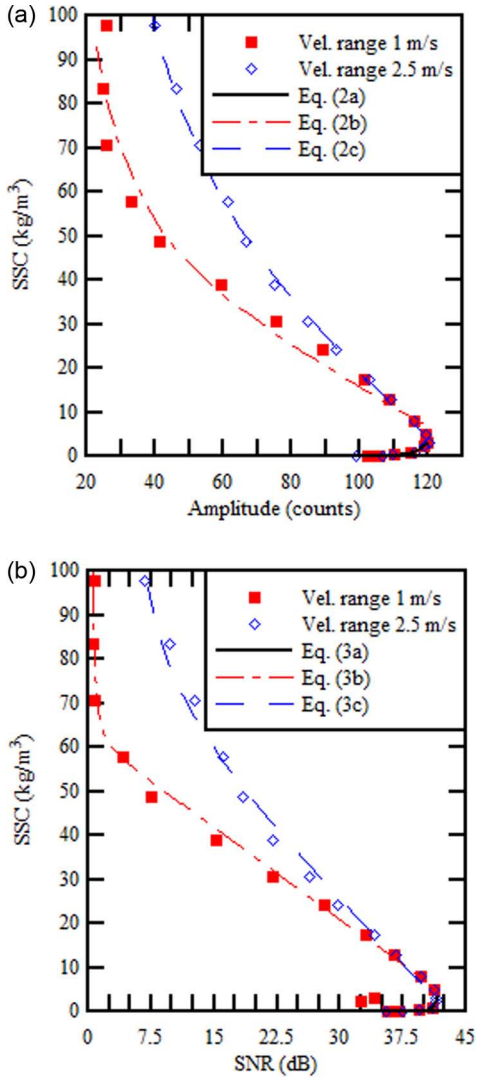

Figure 7. Relationship between suspended sediment concentration, acoustic signal amplitude, and signal-to-noise ratio with the sediment mud collected along Gardens Point Road. (a) Relationship between suspended sediment concentration (SSC in kg m^{-3}) and acoustic signal amplitude (Ampl in counts). Comparison between data and equations (2). (b) Relationship between suspended sediment concentration (SSC in kg m^{-3}) and SNR (dB). Comparison between data and equation (3).

[15] The ADV unit was placed at two closely located sites where the ADV sampling volume was at 0.35 and 0.083 m above the bed (Table 1, column 7). Both sites are highlighted in Figures 4b and 4c. Figure 8 presents the time variations of instantaneous longitudinal velocity and the data are compared with the water elevations of the Brisbane River at the City Gauge located 1.55 km downstream. In Figure 8, the invert elevation (3.42 m AHD) at the sampling site is shown with a horizontal dashed line using the same vertical scale as the City Gauge water elevation data. The longitudinal velocity data illustrated some large fluctuations around a mean trend (thick black line) throughout the study period. The magnitude of longitudinal velocity was about 0.5 m s^{-1}, all except during the last data set T5 (Table 4, column 7). For comparison, the longitudinal velocity in the main channel of the Brisbane River was estimated to be between 3.5 and 4.5 m s^{-1} at the peak of the flood (T. Malone, personal communication, 2011). During the last data set T5, the water level dropped rapidly from 0.26 m down to less than 0.10 m when the ADV unit came to be out of the water. The velocity data showed a very slow motion implying that the inundation flow was disconnected from the main river channel.

[16] The large fluctuations of all velocity components were caused by slow oscillations with dominant periods of about 60 to 100 s, as illustrated in Figure 9 for the longitudinal velocity component. The characteristic period was close to the first mode of natural sloshing resonance of the water body, linked with the C block car park length [*Brown et al.*, 2011]. It is believed that the flow constriction created by the concrete stairwells seen in Figure 4c induced some choking. The gap between stairwells was 10 m compared to the car park width of 33.6 m. When the flow in the stairwell contraction choked, the energy losses in the contraction became substantially larger than the rate of energy loss of the main flow, and the inundation flow would redirect around the stairwells to achieve a minimum energy path. The pattern yielded some flow instabilities in the surroundings of stairwells which could be amplified when their period was close to the natural sloshing period of the building car park [*Brown et al.*, 2011].

[17] There were a small number of suspended sediment sampling undertaken in the Brisbane River catchment during the early part of the flood event. The data yielded SSC = 4.5 kg m^{-3} on 7 January 2011 at Gregors Creek (upper Brisbane Valley), 10.3 kg m^{-3} on 11 January 2011 at Adam's Bridge (Bremer Valley), and 19.1 kg m^{-3} on 11 January 2011 at Tenthill (Lockyer Valley) [*Event Monitoring Group*, 2011; *Grinham et al.*, 2012]. The sampling stations are shown in Figure 1a. Both the Lockyer Creek and Bremer River discharged into the Lower Brisbane River upstream of the City of Brisbane, and their courses are undammed. The suspended sediment samples were collected manually and from automatic samplers, and the data were restricted to the rising limb of the flood hydrograph because of subsequent equipment failures and inaccessibility of the flooded sites. Only the last two samples were collected during the rising limb of the main flood event and these SSC data were of the same order of magnitude as the SSC values deduced from the ADV signal amplitude during the rising limb of the flood hydrograph in Brisbane (Figure 10a, left side). Furthermore, during large floods similar to the present investigation, the Brisbane River water was murky and some suspended sediment load extrapolation would predict SSCs in excess of 3 kg m^{-3} [*Horn et al.*, 1998, 1999]. On 12 and 13 January 2011, the flood water was very turbid when the authors went into the water at Gardens Point Road. With a crude analogy with the Secchi disk method, they could not see their fingers about 2–3 cm below the water surface which corresponded to SSCs greater than 5 to 25 kg m^{-3} during the laboratory tests. Lastly, the calculations based upon equation (2a) would yield SSC values within 1 to 1.5 kg m^{-3} during the rising limb of the hydrograph (samples T1 and T2). Such values would seem low compared to the observations in the Lockyer and Bremer Valleys during the rising stage of the flood. More the calculations based upon equation (2a) would

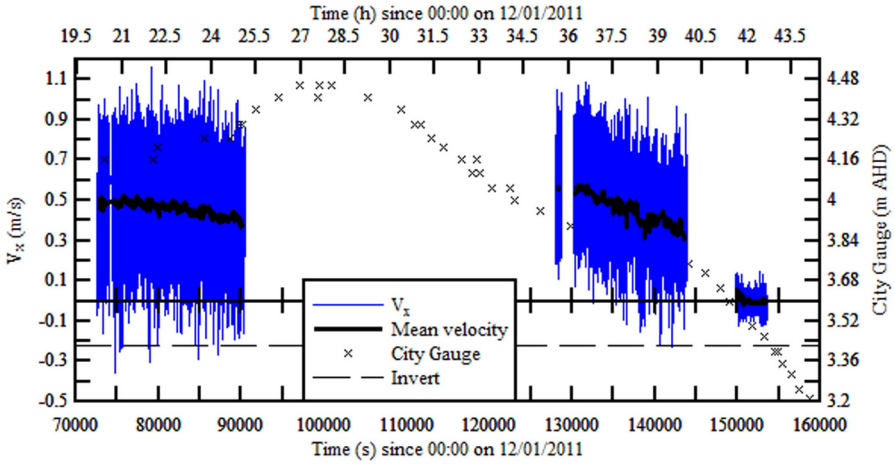

Figure 8. Time variations of the longitudinal velocity V_x along Gardens Point Road during the January 2011 flood. Comparison with the Brisbane River City Gauge data. The dashed line indicates the bed elevation at the sampling sites (nearly identical for locations A and B).

yield negative (meaningless) SSC values during the falling limb of the hydrograph (samples T3, T4, and T4) since the signal amplitude values were typically below 90 to 95 counts. All these suggested that the SSCs were greater than 3 kg m^{-3} in Gardens Point Road on 12–14 January 2011, and equations (2b) and (2c) were representative of the relationship between the suspended sediment concentration (SSC) and signal amplitude (Ampl).

[18] The time variations of suspended sediment concentration SSC and longitudinal suspended sediment flux q_s = SSC × V_x are presented in Figure 10. In Figure 10 each graph includes the instantaneous data and the mean values, as well as the City Gauge data for comparison. The suspended sediment concentration data showed a general trend with an increase in mean concentration from about 6 to more than 20 kg m^{-3} during the entire study period (Figure 10a and Table 4 (column 10). These values were comparable to the sediment sampling observations in the Lockyer and Bremer Valleys during the rising stage of the flood (see above). The present data trend might be linked with the change in ADV sampling volume elevation between locations A and B. During the test T5 with shallow waters, it is likely that the data reflected an increase in SSC prior to mud deposition on the concrete invert. The SSC data highlighted some large and rapid fluctuations in sediment concentration (Figure 10a). The SSC fluctuations were dominated with high-frequency fluctuations, corresponding to periods less than 3 s.

[19] During the data series T4 on Thursday afternoon of 13 January 2011, the suspended sediment concentration estimates highlighted two unusual features. First, some large suspended sediment concentrations and large fluctuations in SSC about the mean trend were observed between t = 135,600 and 140,800 s, i.e., on 13 January between 13:40 and 15:10. The period corresponded to an unusual flow pattern with changes in longitudinal flow direction by up to 12° at the sampling point. It is conceivable that the development of large-scale vortical structures could have enhanced turbulent mixing and resuspended some deposited sediment materials at the time. The passage of debris and some form of upstream blockage induced by debris might be a plausible explanation for the large suspended sediment concentrations and longitudinal flow direction shift. The possibility of some stratification of the water column at the sampling site might not be discounted, although visual observations in the Brisbane River main channel indicated some murky surface waters during the same period. Second, another feature was the existence of long-period oscillations in terms of suspended sediment concentration with a period of about 1100 s (18 min) (Figure 10a). Such

Table 4. Velocity and Suspended Sediment Concentration Measurements Along Gardens Point Road on 12–13 Jan 2011[a]

Data File	ADV Location	Sampling Rate (Hz)	Velocity Range (m s^{-1})	z (m)	No. of Samples	Average V_x (m s^{-1})	Average V_y (m s^{-1})	Average V_z (m s^{-1})	Average SSC (kg m^{-3})	Average SSC × V_x (kg m^{-2} s^{-1})
T1	**A**	**50**	**2.5**	**0.350**	**70,162**	**0.487**	**−0.0024**	**0.533**	**5.45**	**2.67**
T2	A	50	2.5	0.350	800,000	0.455	0.00053	0.486	6.03	2.73
T3	**B**	**50**	**2.5**	**0.083**	**31,171**	**0.565**	**−0.0159**	**0.179**	**19.81**	**11.57**
T4	B	50	1.0	0.083	685,884	0.452	0.001	0.129	22.1	9.18
T5	B	50	1.0	0.083	196,762	0.00176	−0.0002	0.00438	27.28	0.085

[a]Average is time average over the test sampling duration. Location A: ADV unit mounted horizontally on boom gate support. Location B: ADV unit mounted vertically on a hand rail. SSC: Suspended sediment concentration. V_x: Longitudinal velocity component. V_y: Transverse horizontal velocity component. V_z: Vertical velocity component. Bold data: Data set with relatively small number of samples.

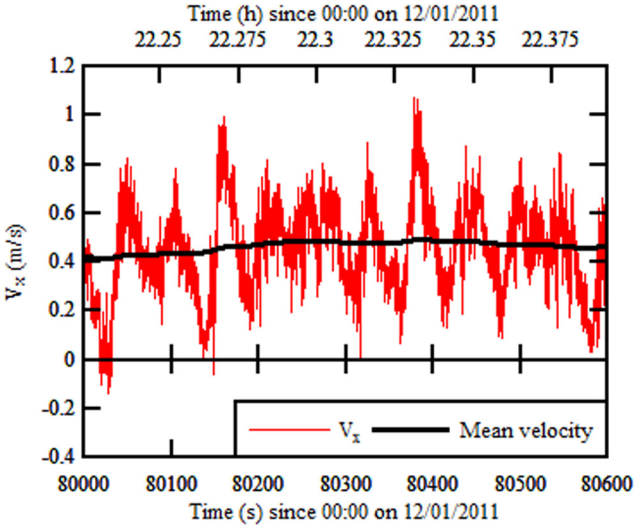

Figure 9. Time variations of the longitudinal velocity V_x during the data set T2 along Gardens Point Road during the January 2011 flood. The comparison between instantaneous data and mean trend over 600 s highlights the long-periods in terms of longitudinal velocity.

oscillations were not seen in the velocity data (Figure 8), and the authors do not have any physical explanation.

[20] The longitudinal suspended sediment flux data $q_s = \text{SSC} \times V_x$ showed some substantial sediment flux values which would be consistent with the murky color of the Brisbane River (Figure 10b). On average, q_s ranged from 2.5 to 11 kg s^{-1} m^{-2}. Herein q_s represents a sediment flux per unit area at the sampling location. The results highlighted some large fluctuations in suspended sediment flux per unit area during the study about the peak of the flood (Figure 10b). Furthermore, the data showed a major increase in sediment flux about t = 136,263 s (13 January at 13:51) (Figure 10b). It is believed to be linked with the high values of SSC observed at the time. During the data series T5, the sediment flux data indicated some low flux values despite some large SSCs. This series corresponded to a period of very sluggish flow motion (Table 4, column 7), likely associated with sediment deposition on the invert.

[21] The turbulent kinetic energy TKE was estimated as

$$\text{TKE} = \frac{1}{2}(v_x^2 + v_y^2 + v_z^2), \tag{3}$$

where the velocity fluctuation v was the velocity deviation from a mean velocity $\langle V \rangle$ calculated as the low-pass filtered velocity data with a cut-off frequency of 0.002 Hz (1/500 s^{-1}):

$$v = V - \langle V \rangle. \tag{4}$$

[22] For example, both V_x and $\langle V_x \rangle$ are shown in Figure 9. Herein the velocity fluctuation v, hence the turbulent kinetic energy, encompassed both the slow fluctuating motion and the turbulent motion [*Brown and Chanson*, 2013]. The turbulent kinetic energy and its mean value are presented in Figure 10c. The mean TKE was calculated as

$$\overline{\text{TKE}} = \frac{1}{2}(\overline{v_x^2} + \overline{v_y^2} + \overline{v_z^2}), \tag{5}$$

with the averaging being calculated over a 500 s interval (25,000 data samples). The TKE data, as well as the fluctuations of all three velocity components (not shown), did not show any anomalies around the time of sediment concentration and flux spikes which might explain the physical data.

4. Discussion

[23] Despite some manufacturers' recommendations [e.g., *Sontek*, 2008], *Salehi and Strom* [2011] argued that the signal-to-noise ratio (SNR) may be used as a surrogate measure for SSC. For the present tests, the relationship between SSC and SNR is shown in Figure 7b, illustrating similar features to the relationship between SSC and signal amplitude. The data were best correlated by

$$\begin{gathered}\text{SSC} = 2.86 \times 10^{-8} \times (\text{SNR} - 35.6)^{10.4}, \\ \text{SSC} \leq 3.2\,\text{kg m}^{-3},\end{gathered} \tag{6a}$$

$$\begin{gathered}\text{SSC} = 62.45 - 1.385 \times \text{SNR} + \frac{11.27}{\text{SNR}^2}, \\ \text{SSC} > 3.2\,\text{kg m}^{-3} - \text{Velocity Range} : 1.0\,\text{m s}^{-1},\end{gathered} \tag{6b}$$

$$\begin{gathered}\text{SSC} = 82.22 - 1.938 \times \text{SNR} + \frac{1458}{\text{SNR}^2}, \\ \text{SSC} > 3.2\,\text{kg m}^{-3} - \text{Velocity Range} : 2.5\,\text{m s}^{-1},\end{gathered} \tag{6c}$$

where SNR is in decibels, with a normalized correlation coefficient of 0.961, 0.977, and 0.997 respectively. Equations (6) are compared with the data in Figure 7b. Equations (6b) and (6c) were tested and compared against equations (2b) and (2c), respectively, for the entire field data set. The calculations showed close results both qualitatively and quantitatively in terms of the SSC estimates based upon the signal amplitude and SNR (Figure 11). Figure 11 presents a comparison for the whole data set. The SSC estimates were very close during the rising limb of the hydrograph (ΔSSC < 0.13 kg m^{-3} on average). During the falling part of the flood hydrograph, the SSC estimates based upon the SNR (equations (6)) tended to overestimate the SSC by about +3 kg m^{-3}, compared to the SSC estimates derived from the signal amplitude (equations (2)). Simply the SNR might be a suitable SSC surrogate for the present data set.

[24] Some statistical properties in terms of suspended sediment concentration SSC and flux per unit area q_s are presented in Table 4 (columns 10 and 11). Altogether the physical data highlighted some significant sediment load with large SSCs and suspended sediment fluxes per unit area. Figure 12 presents the suspended sediment load per unit area data as functions of the suspended sediment concentrations. The present time-averaged data were compared with physical data recorded in rivers during floods and in estuaries (Table 5 and Figure 12). Table 5 regroups a

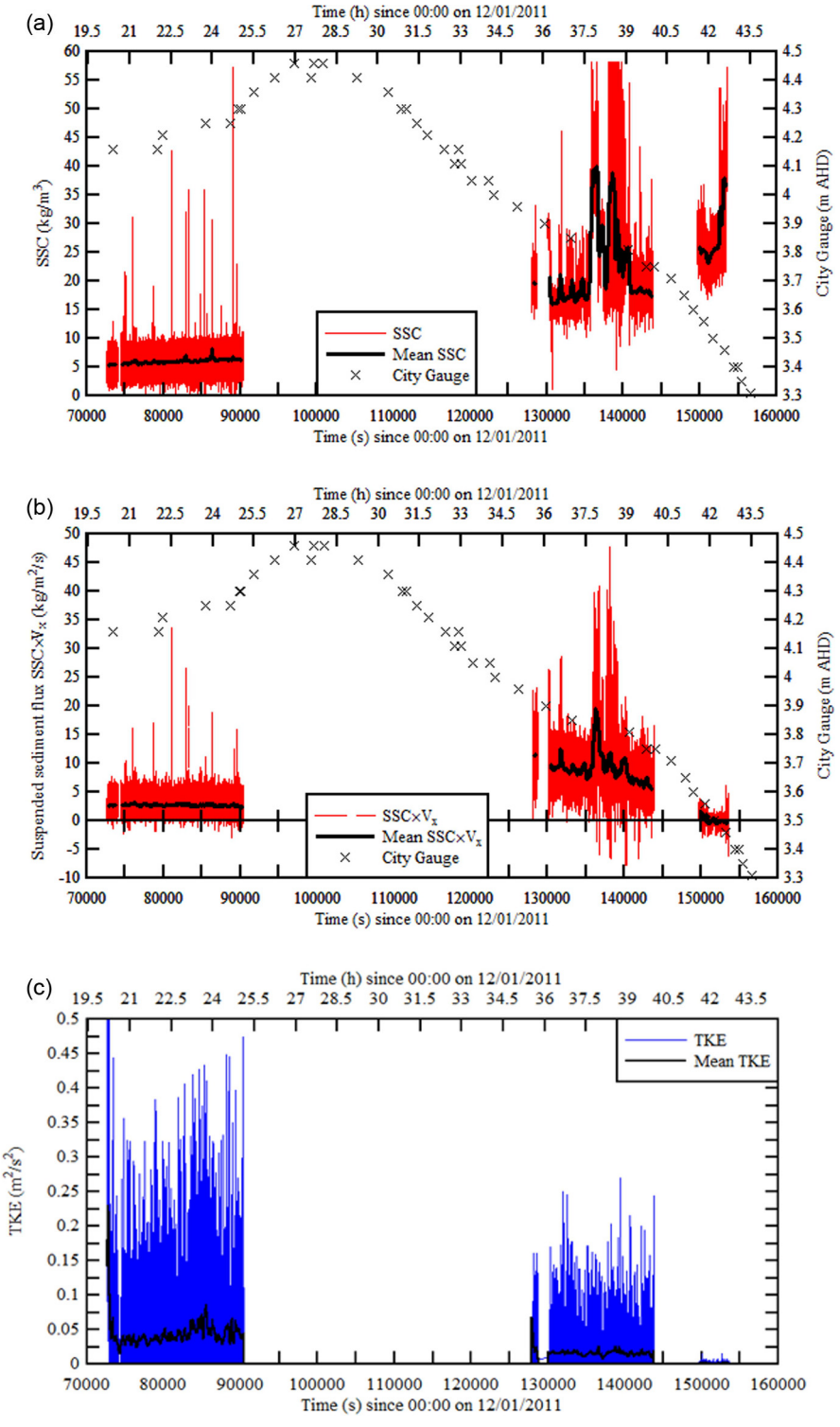

Figure 10. Time variations of suspended sediment concentration SSC, suspended sediment flux q_s = SSC × V_x and turbulent kinetic energy TKE along Gardens Point Road during the January 2011 flood. (a) Suspended sediment concentration SSC. (b) Suspended sediment flux q_s = SSC × V_x. (c) Turbulent kinetic energy TKE.

number of field observations of suspended sediment loads in rivers in flood, including in the Amazon, Mississippi, and Nile Rivers, as well as hyperconcentrated flow data (Yellow River, North Fork Toutle River). Figure 12 shows high suspended sediment fluxes per unit area and SSC data in the Brisbane River during the January 2011 flood. While larger values were measured in hyperconcentrated flows and behind a tidal bore (Garonne River) in an estuary, the

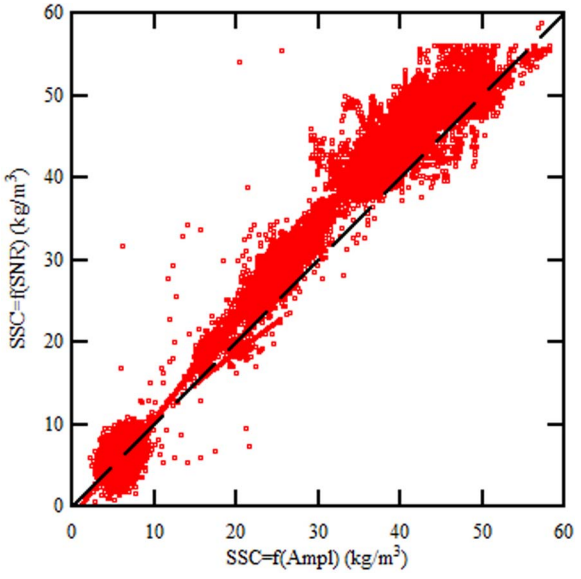

Figure 11. Suspended sediment concentration SSC estimates based upon the SNR (equations (6b) and (6c)) as a function of SSC derived from the signal amplitude (equations (2b) and (2c)) along Gardens Point Road during the January 2011 flood for the whole data set (1,629,208 samples).

present findings implied higher suspended sediment concentrations and fluxes than in many other river floods. The present results were further consistent with the earlier findings of *Horn et al.* [1999] during floods in Queensland rivers.

[25] Using bentonite suspensions with 5% mass concentration, *Chanson et al.* [2006a] highlighted a non-Newtonian thixotropic flow behavior using both dam break wave experiment and rheometry tests. Similarly *Coussot and Ovarlez* [2010] showed the non-Newtonian thixotropic behavior of bentonite suspensions with volume concentrations between 3% and 7% based upon direct magnetic resonance imaging (MRI) observations, and their data trend hinted a non-Newtonian behavior for mass concentrations as low as 1%. During the present field study, SSC estimates between 5 and 60 kg m^{-3} were recorded (Figure 10a), corresponding to volume concentrations between 0.2% and 2.3%, and mass concentrations between 0.5 and 6%. The present findings indicated some high suspended sediment concentration levels together with the rheological data, for which a non-Newtonian flow behavior could be expected.

[26] Importantly the present data were point measurements. They should not be extrapolated to the main river channel or any other floodplain sections. When the authors were in the water on the evening of Wednesday 12 January and Thursday 13 January to install and later relocate the ADV unit, the car park invert was bare concrete. There was no sediment deposit, no bed form, or any form of bed load motion. Owing to the relatively fast and turbulent motion, the sediment motion was dominated by sediment suspension.

[27] It may be stressed that the present field data set was obtained under very difficult conditions when the Brisbane city and its business district were locked out, access to most field equipment was extremely difficult, and the field deployment started before the peak of the flood at a time of conflicting forecasts in terms of the highest water level (by up to 1 m).

5. Conclusion

[28] During the January 2011 flood of the Brisbane River in Brisbane (Australia), a field investigation was conducted in an inundated urban environment, and a number of flood water deposit samples and velocity data were collected.

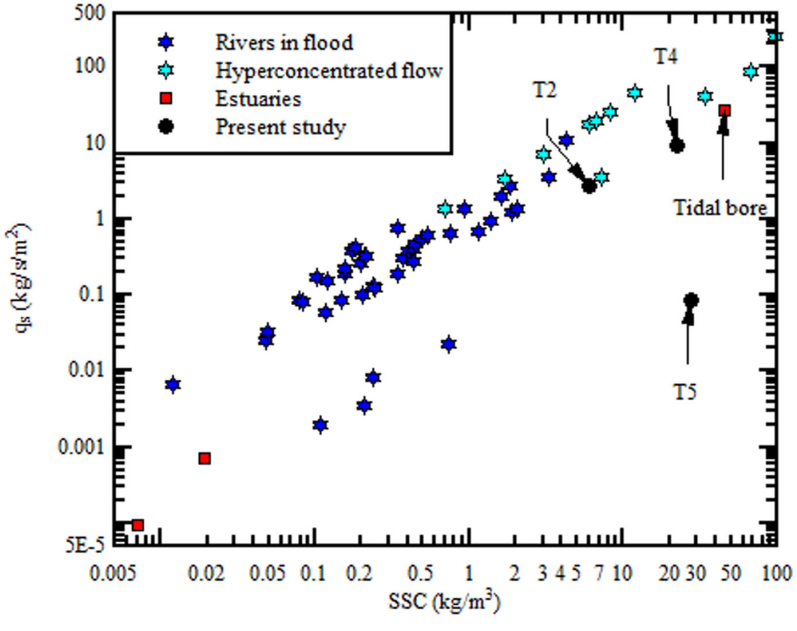

Figure 12. Suspended sediment flux q_s (kg s^{-1} m^{-2}) as a function of the suspended sediment concentration SSC. Comparison between present data (periods T2, T4, and T5), observations in rivers during flood, and data in estuaries (Table 5).

Table 5. Measurements of Suspended Sediment Concentrations and Suspended Sediment Flux per Unit Area in Rivers During Floods and in Estuaries

Reference	River	Location	Date (dd/mm/yyyy)	Q ($m^3 s^{-1}$)	V ($m^3 s^{-1}$)	SSC ($kg m^{-3}$)	q_s ($kg s^{-1} m^{-2}$)	Remarks
Rivers								
Bouchez et al. [2011]	Solimoes (Brazil)	Manacapuru	1/03/2006	109,200	–[a]	0.237	0.008352	b
	Madeira (Brazil)	Foz Madeira	1/03/2006	47,200	–	0.738	0.022834	b
	Amazonas (Brazil)	Iracema	1/03/2006	134,500	–	0.108	0.001948	b
	Amazonas (Brazil)	Obidos	1/03/2006	168,900	–	0.211	0.003508	b
Horn et al. [1998]	Fitzroy (Australia)	Laurel Banks	12/03/1994	2,700	1.07	3.3	3.53	b
	Brisbane (Australia)	College Crossings	5/05/1996	1,984	–	0.925	1.35	b
Van Den Berg and Van Gelder [1993]	Huanghe (China)	Li-Jin	2/09/1987	1,212	1.30	68.02	88.45	Hyperconcentrated flow[c]
	Huanghe (China)	Li-Jin	9/09/1987	1,050	1.2	34.50	41.40	Hyperconcentrated flow[c]
	Huanghe (China)	Li-Jin	22/09/1987	185	0.5	7.21	3.60	Hyperconcentrated flow[c]
Li et al. [1998]	Huanghe (China)	Li-Jin	13/08/1993	2,500	2.6	96.7	250.4	Hyperconcentrated flow[b]
Vanoni [1975]	Missouri (USA)	Omaha (Nebraska)	Oct. 1951	–	2.53	4.3	10.88	b
	Rio Puerco (USA)	Bernado (New Mexico)	19/08/1961	–	1.58	131.2	206.75	Hyperconcentrated flow[b]
Akali [2002]	Mississippi (USA)	Union Point (Mississippi)	27/02/1998	28,624	1.78	0.50	0.559	b
	Mississippi (USA)	Union Point (Mississippi)	23/03/1998	30,110	1.55	0.50	0.546	b
	Mississippi (USA)	Union Point (Mississippi)	10/04/1998	31,368	1.66	0.40	0.380	b
	Mississippi (USA)	Union Point (Mississippi)	17/04/1998	30,282	1.67	0.54	0.620	b
	Mississippi (USA)	Union Point (Mississippi)	8/05/1998	34,544	1.93	0.45	0.464	b
	Mississippi (USA)	Union Point (Mississippi)	9/06/1998	21,344	1.30	0.43	0.394	b
	Mississippi (USA)	Union Point (Mississippi)	3/08/1998	16,195	1.29	0.37	0.304	b
Jordan [1965]	Mississippi (USA)	St Louis, Missouri	17/4/1951	14,753	2.25	0.342	0.750	b
	Mississippi (USA)	St Louis, Missouri	21/5/1951	10,251	1.61	0.206	0.329	b
	Mississippi (USA)	St Louis, Missouri	16/7/1951	19,935	2.21	0.175	0.387	b
	Mississippi (USA)	St Louis, Missouri	22/7/1951	21,606	2.30	0.181	0.418	b
	Mississippi (USA)	St Louis, Missouri	30/7/1951	13,252	1.64	0.102	0.172	b
	Mississippi (USA)	St Louis, Missouri	17/9/1951	10,987	1.53	0.214	0.328	b
	Mississippi (USA)	St Louis, Missouri	24/9/1951	8,070	1.32	0.078	0.087	b
	Mississippi (USA)	St Louis, Missouri	8/10/1951	5,890	1.12	0.120	0.151	b
	Mississippi (USA)	St Louis, Missouri	15/10/1951	5,154	1.02	0.084	0.081	b
	Mississippi (USA)	St Louis, Missouri	13/11/1951	6,201	1.21	0.155	0.187	b
	Mississippi (USA)	St Louis, Missouri	3/12/1951	5,380	1.14	0.155	0.222	b
Pitlick [1992]	North Fork Toutle (USA)	Hoffstadt Creek Bridge	17/02/1989	–	2.96	5.95	17.61	Hyperconcentrated flow[b]
	North Fork Toutle (USA)	Hoffstadt Creek Bridge	10/03/1989	–	3.75	12	45.00	Hyperconcentrated flow[b]
	North Fork Toutle (USA)	Hoffstadt Creek Bridge	21/03/1989	–	2.81	6.76	19.00	Hyperconcentrated flow[b]
	North Fork Toutle (USA)	Hoffstadt Creek Bridge	28/03/1989	–	3.06	8.23	25.18	Hyperconcentrated flow[b]
	North Fork Toutle (USA)	Hoffstadt Creek Bridge	11/04/1989	–	2.35	3.02	7.10	Hyperconcentrated flow[b]
	North Fork Toutle (USA)	Hoffstadt Creek Bridge	21/04/1989	–	1.96	1.7	3.33	Hyperconcentrated flow[b]
	North Fork Toutle (USA)	Hoffstadt Creek Bridge	27/04/1989	–	1.94	0.69	1.34	Hyperconcentrated flow[b]
Buckley [1921]	Nile (Egypt)	Beleida	1/08/1921	906	0.51	0.118	0.0596	c
	Nile (Egypt)	Beleida	13/08/1921	2,571	0.88	0.75	0.663	c
	Nile (Egypt)	Beleida	22/08/1921	4,980	1.24	1.62	2.01	c
	Nile (Egypt)	Khannaq	15/09/1920	7,220	1.48	1.83	2.71	c
	Nile (Egypt)	Khannaq	16/09/1920	6,400	1.32	0.198	0.261	c
	Diversion Channel	Ismailia (Egypt)	1/07/1922	50.5	0.56	0.012	0.00667	c
	Diversion Channel	Ismailia (Egypt)	22/07/1922	47.5	0.52	0.048	0.0251	c
	Diversion Channel	Ismailia (Egypt)	1/08/1922	68.3	0.68	0.0491	0.0333	c
	Diversion Channel	Ismailia (Egypt)	8/08/1922	66	0.64	0.436	0.279	c
	Diversion Channel	Ismailia (Egypt)	15/08/1922	66	0.68	1.38	0.942	c

Table 5. (continued)

Reference	River	Location	Date (dd/mm/yyyy)	Q ($m^3 s^{-1}$)	V ($m^3 s^{-1}$)	SSC ($kg m^{-3}$)	q_s ($kg s^{-1} m^{-2}$)	Remarks
	Diversion Channel	Ismailia (Egypt)	19/08/1922	66	0.68	2.05	1.40	c
	Diversion Channel	Ismailia (Egypt)	9/09/1922	62.5	0.64	1.88	1.21	c
	Diversion Channel	Ismailia (Egypt)	7/10/1922	53.3	0.59	1.16	0.683	c
	Diversion Channel	Ismailia (Egypt)	25/11/1922	51.5	0.55	0.344	0.189	c
	Diversion Channel	Ismailia (Egypt)	2/12/1922	42.9	0.50	0.244	0.121	c
	Diversion Channel	Ismailia (Egypt)	9/12/1922	49.9	0.55	0.236	0.130	c
	Diversion Channel	Ismailia (Egypt)	16/12/1922	42.9	0.50	0.202	0.100	c
	Diversion Channel	Ismailia (Egypt)	20/12/1922	55.5	0.59	0.147	0.086	c
Estuaries								
Trevethan et al. [2007]	Eprapah (Australia)	Site 3	5–7/6/2006	–	–	0.0071	9.37×10^{-5}	d,e
Chanson et al. [2006b]	Eprapah (Australia)	Site 2B	16–18/5/2005	–	–	0.0190	0.000732	d,e
Chanson et al. [2011]	Garonne (France)	Arcins	11/09/2010	–	–	46.02	26.33	Tidal Bore[d,e]
Present study								
2011 flood	Brisbane (Australia)	Gardens Pt	12/1/2011	–	0.46	6.03	2.73	d
	Brisbane (Australia)	Gardens Pt	13/1/2011	–	0.45	22.1	9.18	d
	Brisbane (Australia)	Gardens Pt	13/1/2011	–	0.0018	27.3	0.085	d

[a] –: Data not available.
[b] Depth-averaged data.
[c] Data measured close to the bed.
[d] Point measurement data.
[e] Time-averaged flux amplitude.

The sediment material was cohesive with a typical particle size of about 25 μm, and the mud sludge exhibited a non-Newtonian behavior. Some experiments under controlled conditions were performed to use the acoustic backscatter amplitude of an ADV as a surrogate estimate of the suspended sediment concentration (SSC), although the data suggested the signal-to-noise ratio (SNR) to be also a valid proxy. The laboratory data showed that the relationship between SSC and backscatter amplitude had two distinct trends: a monotonic increase of SSC with signal amplitude for SSC < 3 kg m^{-3}, and a decrease in backscatter amplitude with increasing SSC for large suspended loads.

[29] The field measurements were conducted in the inundated urban setting about the peak of the Brisbane River flood with the microADV system. The data set yielded the instantaneous velocity, suspended sediment concentrations, and suspended sediment flux per unit area at the sampling site in the inundated urban setting. The suspended sediment concentration (SSC) estimates showed a general trend with increasing SSC for decreasing water depth: the mean suspended concentration increased from 6 to more than 20 kg m^{-3} during the study period. The suspended sediment flux data highlighted some substantial sediment flux values consistent with the murky appearance of floodwaters. The end of the study was marked by a period of very slow flow motion when sediment deposition on the invert likely took place. During a data series (T4), some long-period oscillations were observed with a period of about 18 min, although the cause of these oscillations remains unknown to the authors. Altogether the field data set implied very significant levels of SSC and suspended sediment flux in the Brisbane River.

[30] It must be noted that the present study highlighted a number of limitations. The results were obtained at a site in a complicated urban environment. Different results might have been observed at other flooded locations and in the main river channel. The calibration curve was specific to the microADV unit at the time of the tests. Lastly, the field deployment was conducted in very challenging conditions. These included the preparation and installation of the equipment when most services were shut down and many city streets were under water, during a period when nearly 150,000 people were affected by the flood in Brisbane.

[31] **Acknowledgments.** The writers thank Dave McIntosh and Jay Madhani for their assistance during the tests and field deployment. They acknowledge Jon James, Gary Woods, and QUT Security for access to tools, instrumentation, and generators, and site access during the stressful and busy period of the flood. They acknowledge also Frank Shi (Julius Kruttschnitt Mineral Research Centre) for sediment material testing, and Nathaniel Raup (QUT) for sediment organic content measurements. They thank all people who participated in the field works and those who assisted in the postfield work calibration of the ADV sediment concentration. The first writer also acknowledges the financial support of QUT Faculty of Built Environment and Engineering through a special project grant. The second writer acknowledges the financial support of the Australian Research Council (grant DP120100481). The authors acknowledge some helpful comments from Frédérique Larrarte (IFSTTAR, Bouguenais, France), Alistair Grinham (University of Queensland), as well as from the reviewers.

References

Akalin, S. (2002), Water temperature effect on sand transport by size fraction in the lower Mississippi, Ph.D. thesis, Colorado State University, Fort Collins, CO, 243 pp.

Antoine, P., A. Giraud, M. Meunier, and T. Van Asch (1995), Geological and geotechnical properties of the "Terres Noires" in southeastern France: Weathering, erosion, solid transport and instability, *Eng. Geol.*, *40*, 223–234.

BOM (2011a), Frequent heavy rain events in late 2010/early 2011 lead to widespread flooding across eastern Australia, *Special Climate Statement 24*, National Climate Centre, Bureau of Meteorology, Melbourne VIC, Australia, Revision b, 23 January 2011, 28 pp.

BOM (2011b), Monthly Weather Review. Queensland. January 2011, *Monthly Weather Review*, Bureau of Meteorology, Melbourne VIC, Australia, 45 pp.

Bouchez, J., F. Metivier, M. Lipker, L. Maurice, M. Perez, J. Gaillardet, and C. France-Lanord (2011), Prediction of depth-integrated fluxes of suspended sediment in the Amazon River: Particle aggregation as a complicating factor, *Hydrolog. Processes*, *25*, pp. 778–794, doi:10.1002/hyp.7968.

Brown, R., and H. Chanson (2013), Turbulence and suspended sediment measurements in an urban environment during the Brisbane River flood of January 2011, *J. Hydraul. Eng.*, *139*, doi:10.1061/(ASCE)HY.1943-7900.0000666, in press.

Brown, R., H. Chanson, D. McIntosh, and J. Madhani (2011), Turbulent velocity and suspended sediment concentration measurements in an urban environment of the Brisbane River flood plain at Gardens Point on 12–13 January 2011, *Hydraulic Model Report No. CH83/11*, School of Civil Engineering, The University of Queensland, Brisbane, Australia, 120 pp.

Buckley, A. B. (1921), The influence of silt on the velocity of flowing water in open channels, *Min. Proc. Inst. Civil Eng. UK*, *216*(1922–1923), 183–211.

Chanson, H. (2004), *The Hydraulics of Open Channel Flow: An Introduction*, 2nd ed., 630 pp., Butterworth-Heinemann, Oxford, UK.

Chanson, H. (2011), The 2010–2011 floods in Queensland (Australia): Observations, first comments and personal experience, *J. Houille Blanche*, *1*, 5–11.

Chanson, H., S. Jarny, and P. Coussot (2006a), Dam break wave of thixotropic fluid, *J. Hydraul. Eng.*, *132*(3), 280–293, doi:10.1061/(ASCE)0733-9429(2006)132:3(280).

Chanson, H., M. Takeuchi, and M. Trevethan (2006b), Using turbidity and acoustic backscatter intensity as surrogate measures of suspended sediment concentration. Application to a sub-tropical estuary (Eprapah Creek), *Report No. CH60/06*, Div. of Civil Engineering, The University of Queensland, Brisbane, Australia, Aug, 44 pp.

Chanson, H., M. Takeuchi, and M. Trevethan (2008), Using turbidity and acoustic backscatter intensity as surrogate measures of suspended sediment concentration in a small sub-tropical estuary, *J. Environ. Manage.*, *88*(4) 1406–1416, doi:10.1016/j.jenvman.2007.07.009.

Chanson, H., D. Reungoat, B. Simon, and P. Lubin (2011), High-frequency turbulence and suspended sediment concentration measurements in the Garonne River tidal bore, *Estuar. Coastal Shelf Sci.*, *95*(2–3), 298–306, doi:10.1016/j.ecss.2011.09.012.

Coussot, P. (1997), Mudflow rheology and dynamics, *IAHR Monogr.*, Balkema, The Netherlands.

Coussot, P., and G. Ovarlez (2010), Physical origin of shear-banding in jammed systems, *Eur. Phys. J. E*, *33*(3), 183–188, doi:10.1140/epje/i2010-10660-9.

Event Monitoring Group (2011), South East Queensland event monitoring summary (6th–16th January 2011). Preliminary suspended sediment solid loads calculations, *South East Queensland Event Monitoring (Water Quality and Aquatic Ecosystem Heath)*, Queensland Department of Environment and Resource Management, Australia, 4 pp.

Fugate, D. C., and C. T. Friedrichs (2002), Determining concentration and fall velocity of estuarine particle populations using ADV, OBS and LISST, *Cont. Shelf Res.*, *22*, 1867–1886.

Graf, W. H. (1971), *Hydraulics of Sediment Transport*, McGraw-Hill, New York.

Grinham, A., B. Gibbes, D. Gale, A. Watkinson, and M. Bartkow (2012), Extreme rainfall and drinking water quality: A regional perspective, *Proc. Water Pollut. 164*, 183–194, doi:10.2495/WP120161.

Ha, H. K., W. Y. Hsu, J. P. Y. Maa, Y. Y. Shao, and C. W. Holland (2009), Using ADV backscatter strength for measuring suspended cohesive sediment concentration, *Cont. Shelf Res.*, *29*, 1310–1316.

Horn, A., M. Joo, and W. Poplawski (1998), Queensland riverine sediment transport rates. A progress report, *Water Quality Group Report No. 2/98*, Queensland Department of Natural Resources, Brisbane, Australia, 48 pp.

Horn, A., M. Joo, and W. Poplawski (1999), Sediment transport rates in highly episodic river systems: A preliminary comparison between empirical formulae and direct flood measurements, *Proc. Water 99 Joint Congress, 25th Hydrology & Water Res. Symp., and 2nd Intl Conf. Water Res. & Environ. Research*, Inst. of Eng., Brisbane, Australia, Vol. 1, pp. 238–243.

Huang, X., and M. Garcia (1998), A Herschel-Bulkley model for mud flow down a slope." *J. Fluid Mech.*, *374*, 305–333.

Jordan, P. R. (1965), Fluvial sediment of the Mississippi River at St. Louis, Missouri, *Geological Survey Water-Supply Paper* 1802, USGS, Washington, DC, 98 pp.

Julien, P. Y. (1995), *Erosion and Sedimentation*, 280 pp., Cambridge University Press, Cambridge, UK.

Li, G., H. Wei, T. Han, and Y. Chen (1998), Sedimentation in the Yellow River delta, Part I: Flow and suspended sediment structure in the upper distributary and the estuary, *Marine Geol.*, *149*, 93–111.

McLelland, S. J., and A. P. Nicholas (2000), A new method for evaluating errors in high-frequency ADV measurements, *Hydrol. Processes*, *14*, 351–366.

Morris, P. H., and D. A. Lockington (2002), Geotechnical compressibility and consolidation parameters and correlations for remoulded fine-grained marine and riverine sediments, *Research Report*, CRC Sustainable Tourism, Queensland, Australia, 51 pp.

Nikora, V., and D. Goring (2002), Fluctuations of suspended sediment concentration and turbulent sediment fluxes in an open-channel flow, *J. Hydraul. Eng.*, *128*(2), 214–224.

Ntelekos, A. A., J. A. Smith, M. L. Baeck, W. F. Krajewski, A. J. Miller, and R. Goska (2008), Extreme hydrometeorological events and the urban environment: dissecting the 7 July 2004 thunderstorm over the Baltimore MD metropolitan region, *Water Resour. Res.*, *44*, W08446, doi:10.1029/2007WR006346.

Otsubo, K., and K. Muraoko (1988), Critical shear stress of cohesive bottom sediments, *J. Hydraul. Eng.*, *114*(10), 1241–1256.

Pitlick, J. (1992), Flow resistance under conditions of intense gravel transport, *Water Resour. Res.*, *28*(3), 891–903.

Roussel, N., R. Le Roy, and P. Coussot (2004), Thixotropy modelling at local and macroscopic scales, *J. Non-Newtonian Fluid Mech.*, *117*(2–3), 85–95.

Salehi, M., and K. Strom (2011), Using velocimeter signal to noise ratio as a surrogate measure of suspended mud concentration, *Cont. Shelf Res.*, *31*, 1020–1032, doi:10.1016/j.csr.2011.03.2008.

Schumacher, B. A. (2002), Methods for the determination of total organic carbon (TOC) in soils and sediments, *US EPA paper NCEA-C-1282, EMASC-001*, U.S. Environmental Protection Agency, Washington, DC, 23 pp.

Shi, F. (2011), Rheological and sizing analysis of Brisbane flood sediment samples collected by QUT, *Technical Rep.*, JKMRC, Brisbane, Australia, 6 pp.

Shi, F., and T. J. Napier-Munn (1996), Measuring the rheology of slurries using an on-line viscometer, *Int. J. Miner. Process*, *47*, 153–176.

Sontek (2008), *16-MHz microADV expanded description*, Sontek/YSI, San Diego, CA, 4 pp.

Trevethan, M., H. Chanson, and M. Takeuchi (2007), Continuous high-frequency turbulence and sediment concentration measurements in an upper estuary, *Estuar. Coastal Shelf Sci.*, *73*(1–2), 341–350, doi:10.1016/j.ecss.2007.01.014.

Van Den Berg, J. H., and A. Van Gelder (1993), Prediction of suspended bed material transport in flows over silt and very fine sand, *Water Resour. Res.*, *29*(5), 1393–1404.

Vanoni, V. (1975), *Sedimentation Engineering*, ASCE, New York.

Voulgaris, G., and S. T. Meyers (2004), Temporal variability of hydrodynamics, sediment concentration and sediment settling in a tidal creek, *Cont. Shelf Res.*, *24*, 1659–1683.

Wang, Z. Y., P. Larsen, and W. Xiang (1994), Rheological properties of sediment suspensions and their implications, *J. Hydraul. Res.*, *32*(4), 495–516.

Wilson, S. D. R., and S. L. Burgess (1998), The steady, spreading flow of a rivulet of mud, *J. Non-Newtonian Fluid Mech.*, *79*, 77–85.

Yevjevich, V. (1992), Water and civilization, *Water Int.*, *17*(4), 163–171.